Upgraded reduction technique for dynamic analysis of structures with friction contact

Upgraded Reduction Technique for Dynamic Analysis of Structures with Friction Contact

F. Mashayekhi* and S. Zucca†
Polytechnic University of Turin, 10129 Turin, Italy
and
A. S. Nobari‡
Imperial College London, London, England SW7 1AL, United Kingdom

https://doi.org/10.2514/1.J059313

A recent reduction technique for the nonlinear forced response analysis of structures with contact interfaces is upgraded. The evaluations of the existing method (Dual formulation), which is based on dual Craig–Bampton method, show its considerable off-line computational time saving because of no matrix manipulation, whereas the resulting reduced model is less accurate than Rubin's in approximating the full finite element model. The accuracy of this formulation is significantly improved with a low additional computational cost in the proposed upgraded formulation. That is obtained by consistent projection of all structural matrices on a reduction basis made up of two sets of vectors: free-interface normal modes and residual flexibility attachment modes. Assembly approach can be considered as dual because the interface forces are kept as generalized coordinates in opposition to primal methods, where interface displacements are retained. To reduce the computational cost, the nonlinear governing equations are also solved in frequency domain using the multiharmonic balance method and alternating frequency time method. Contact elements are introduced between adjacent interface nodes to find the nonlinear contact forces. The performance of the new formulation is demonstrated through two numerical models with friction contact.

Nomenclature

$\boldsymbol{C}$	=	viscous damping matrix of a substructure
E	=	Young's modulus
$\boldsymbol{F}$	=	vector of substructure forces
$\boldsymbol{F}_c$	=	vector of substructure state-dependent nonlinear contact forces
$\boldsymbol{F}_e$	=	vector of a substructure external periodic excitation
$\bar{\boldsymbol{F}}^{(h)}$	=	vector of the hth Fourier coefficients of substructure forces
$\boldsymbol{F}_m$	=	set of a substructure force vector related to master degrees of freedom
$\boldsymbol{F}_s$	=	set of a substructure force vector related to slave degrees of freedom
$\boldsymbol{G}$	=	flexibility matrix of a substructure
$\boldsymbol{K}$	=	stiffness matrix of a substructure
$\boldsymbol{M}$	=	mass matrix of a substructure
n	=	number of substructure degrees of freedom
n_{md}	=	number of static modes
n_{nd}	=	number of nonlinear degrees of freedom
n_{nm}	=	number of normal modes kept in the projection basis
$\boldsymbol{q}$	=	modal amplitude vector
$\boldsymbol{U}$	=	vector of relative displacements at substructure interfaces
$\boldsymbol{X}$	=	vector of substructure displacements
$\bar{\boldsymbol{X}}^{(h)}$	=	vector of the hth Fourier coefficients of substructure displacements
$\boldsymbol{X}_m$	=	set of master degrees of freedom of substructure displacement vector
$\boldsymbol{X}_s$	=	set of slave degrees of freedom of substructure displacement vector
α	=	mass proportional damping coefficient
ζ_p	=	damping ratio associated with the pth free-interface normal mode
μ	=	friction coefficient
ν	=	Poisson's ratio
ρ	=	density
$\boldsymbol{\Phi}$	=	$n \times n_{\text{nm}}$ free-interface normal mode matrix
$\boldsymbol{\phi}_p$	=	mode shape associated with the pth free-interface normal mode
$\boldsymbol{\Psi}$	=	$n \times n_{\text{md}}$ residual flexibility attachment mode matrix
ω	=	frequency of the external excitation force
ω_p	=	natural frequency associated with the pth free-interface normal mode, rad/s

I. Introduction

LOCAL nonlinearity can significantly influence the dynamic behavior of a structure that arises in many applications. In a structure with localized nonlinearity, the restoring force of a portion of the structure depends nonlinearly on the system state due to the presence of cases like local buckling [1], joints [2,3], friction dampers [4,5], and cracks [6,7]. Unfortunately, to capture the dynamic characteristics of such structures, the nonlinear dynamic analysis of a refined finite element (FE) model is required, which is computationally cumbersome. Therefore, model order reduction techniques are of particular interest to speed up the analysis despite the growing capabilities of computers. Friction contact is a common source of local nonlinearity. In addition to frictional interfaces of assembled components, friction dampers are designed frequently to dissipate vibration energy [8]. Load-dependent state of friction contact and slip–stick phenomenon lead to the nonlinear vibration of these structures. Given the complexity of these nonlinear behaviors, several computational methods have been suggested for solution of the resulting nonlinear equations. Direct time integration methods are mainly used to determine the response of systems subjected to transient loads [9]. Numerical integration demands high computational cost for large FE models. When the steady-state response of the system is of interest, frequency-domain

Received 10 December 2019; revision received 11 July 2020; accepted for publication 20 August 2020; published online 30 October 2020.

*Ph.D. Candidate, Department of Mechanical and Aerospace Engineering, Corso Duca degli Abruzzi 24; Fahimeh.mashayekhi@polito.it (Corresponding Author).

†Associate Professor, Department of Mechanical and Aerospace Engineering, Corso Duca degli Abruzzi 24.

‡Professor, Department of Mechanical Engineering, 58 Princes Gate, Kensington.

methods can be applied, allowing for considerable time saving. Among these approximate methods, harmonic balance method (HBM) is one of the extensively used frequency-domain methods [10–13]. Although the HBM reduces the computational effort for large FE models, the computational cost is still expensive because of the large size of the model involved.

Reduced-order models (ROMs) can be employed to reduce the number of governing equations. Primarily developed for linear structures, ROMs are obtained by transforming the physical coordinate system to a generalized coordinate system. Component mode synthesis (CMS) [14] is a very well-known reduction technique involving three steps: decomposing structure into nonoverlapping components, reducing the size of each component by projective reduction, and assembling the ROMs of the components. Component mode synthesis methods, in which the nonlinear degrees of freedom (DOF) (i.e., DOF where friction forces are applied on) can be retained in reduced model, while other DOF can be replaced by generalized coordinates, seem a natural choice for model order reduction of structures with local nonlinearity [2,15–17]. In this way, the CMS-reduced model is able to correctly simulate the different boundary conditions at the contact interfaces (i.e., full stick, gross slip, microslip, lift off, etc.). When the number of interface DOF is large, further reduction can be achieved by means of different approaches: nodeless formulation [18], trial vector derivatives [19], generalized coordinates [20], and adaptive formulation [21].

The CMS methods can be classified depending on the underlying projection basis and assembly techniques. A free-interface base method is proposed in this paper, in which free-interface normal modes and residual flexibility attachment modes constitute the reduced subspace. MacNeal, for the first time, used this subspace as reduction basis and built a ROM [22]. A more accurate model was later proposed by Rubin [23,24]. Rixen also introduced dual Craig–Bampton (DCB) method with free-interface-based modes and a new assembly technique [25]. The assembly of the first two methods, which means that the substructures are assembled using interface displacements and the interface compatibility condition (displacement equality) is a priori satisfied by choosing a unique set of substructure interface DOF. In dual assembly employed in DCB, the substructures are assembled using the interface forces, and the compatibility condition is present explicitly in the assembled equations of motion.

For model order reduction of structures with friction interfaces, Petrov proposed a formulation extracted from the frequency response function (FRF) modification [26]. In this study, an expression is considered for the FRF matrix consisted of a reference FRF matrix and a term describing the FRF matrix variation over the frequency range. A formulation (referred to as Dual formulation in this paper) is also presented in [27], where the formulation is extracted from component-mode synthesis strategy. The comparison of this method with the other free-interface-based methods illustrated its significantly low off-line computational cost corresponding to building the ROM and a higher level of accuracy with respect to conventional modal truncation method. However, the resulting ROM proved [28,29] to be less accurate than Rubin's, which showed the best performances in the case of complex dynamic behavior.

Based on Dual formulation, a new free-interface-based formulation is proposed in this paper for nonlinear forced response analysis of structures with friction contact and referred to as upgraded hybrid reduction (UHR). This formulation allows the same accuracy as Rubin's one, while the off-line computational cost is still low (although higher than the cost of the original dual formulation). The decrease of the computation time necessary to build the ROM is critical in the design iterations of a high-fidelity industrial model, in which ROMs must be generated multiple times, one per each set of structural parameters.

The UHR formulation is described and compared with Rubin's and Dual formulations. Its efficiency and accuracy are demonstrated by forced response analysis of two structures with friction contact in frequency domain using HBM. State-of-the-art contact model is used to model the interface friction behavior, and alternating frequency time (AFT) method is applied to find the Fourier coefficients of nonlinear forces in frequency domain [30]. In Sec. II, these model order reduction techniques are described as well as the nonlinear forced response of structures with friction contacts and the corresponding computational time. In Sec. III, results are presented and discussed.

II. Methodology

All the steps necessary to obtain the ROM of a structure with friction contact for nonlinear forced response analysis are described in this section. The algebraic governing equations are first presented in frequency domain (Sec. II.A). Then, the ROMs of locally nonlinear structures are generated with different reduction techniques (Sec. II.B). Finally, the nonlinear forced response analysis and the computational time of a reduced system analysis are described (Secs. II.B and II.C).

A. Background

1. Governing Equations

A structure, modeled with FE method, is divided into N^s nonoverlapping substructures such that every node belongs to only one substructure and there is friction contact between substructure interfaces. The dynamic equations of motion of a substructure in time domain are as follows:

$$\begin{aligned} \boldsymbol{M}\ddot{\boldsymbol{X}}(t) + \boldsymbol{C}\dot{\boldsymbol{X}}(t) + \boldsymbol{K}\boldsymbol{X}(t) &= \boldsymbol{F}(\boldsymbol{U}, \dot{\boldsymbol{U}}, t) \\ \boldsymbol{F}(\boldsymbol{U}, \dot{\boldsymbol{U}}, t) &= \boldsymbol{F}_e(t) + \boldsymbol{F}_c(\boldsymbol{U}, \dot{\boldsymbol{U}}) \end{aligned} \tag{1}$$

where vectors $\boldsymbol{F}$ and $\boldsymbol{X}$ are $n \times 1$ nodal force and displacement vectors of a substructure with n DOF, respectively; vector $\boldsymbol{U}$ is the relative displacement at the substructure interfaces. Excitation force vector $\boldsymbol{F}_e$ and contact force vector $\boldsymbol{F}_c$ (nonlinearly dependent on the relative displacement and velocity at the interfaces) are both included in nodal force vector $\boldsymbol{F}$. The $n \times n$ matrices $\boldsymbol{M}$, $\boldsymbol{C}$, and $\boldsymbol{K}$ represent the structural mass, viscous damping, and stiffness of the substructure, respectively. The mass proportional damping is also considered as $\boldsymbol{C} = \alpha\boldsymbol{M}$, where α is a constant. The dots refer to time derivatives.

2. Multiharmonic Balance Method

Multiharmonic balance (MHB) method is a useful tool in the forced vibration analysis, where the steady-state part of the solution is of interest. The MHB method turns the differential equations in time domain to a set of algebraic equations in frequency domain. To do this, periodic quantities are approximated by their truncated Fourier series, and then the equilibrium of the Fourier coefficients of each retained harmonic is enforced. Applying the MHB method on the governing equations of motion [Eq. (1)] results in $(H + 1)$ sets of equations at a frequency ω:

$$[-(h\omega)^2\boldsymbol{M} + ih\omega\boldsymbol{C} + \boldsymbol{K}]\bar{\boldsymbol{X}}^{(h)} = \bar{\boldsymbol{F}}^{(h)}(\bar{\boldsymbol{U}}), \quad h = 0,1,...,H \tag{2}$$

where h is the harmonic index; $\bar{\boldsymbol{X}}^{(h)}$ and $\bar{\boldsymbol{F}}^{(h)}$ are the vectors of hth complex Fourier coefficients of $\boldsymbol{X}$ and $\boldsymbol{F}$, respectively. The $n(H + 1) \times 1$ vectors of displacements and forces Fourier coefficients, $\bar{\boldsymbol{X}}$ and $\bar{\boldsymbol{F}}$, include all Fourier coefficients of $\boldsymbol{X}$ and $\boldsymbol{F}$, respectively. Similarly, $\bar{\boldsymbol{U}}$ is the vector of Fourier coefficients of the relative displacements $\boldsymbol{U}$.

B. Model Order Reduction

In this section, three different ROMs, based on the same CMS-based reduction basis, are described: 1) Rubin's method [24], 2) Dual formulation [27], and 3) UHR (the main subject of this paper).

The first step in the CMS model order reduction techniques, as those described in this paper, consists in the definition of two sets of DOF, named master (m) and slave (s) DOF, resulting in a corresponding partition of vectors $\boldsymbol{X}$ and $\boldsymbol{F}$ as

$$\boldsymbol{F} = \begin{bmatrix} \boldsymbol{F}_m \\ \boldsymbol{F}_s \end{bmatrix}, \quad \boldsymbol{X} = \begin{bmatrix} \boldsymbol{X}_m \\ \boldsymbol{X}_s \end{bmatrix} \tag{3}$$

where master DOF are the only physical DOF retained in ROM and slave DOF are projected to reduction basis.

For the ROMs to be suitable for nonlinear forced response analysis, master DOF must include contact DOF, hence referred to as nonlinear (N). In addition, master DOf can also include other DOF, hence referred to as linear (L), corresponding to points of application of the external forces and output DOF at which the response is computed.

It should be noted that for structures with contact interfaces, the relative displacement vector at contact surfaces $\boldsymbol{U}$ can be easily obtained after model order reduction because nonlinear DOF of each substructure are retained in its CMS-reduced model.

The projection basis of free-interface reduction techniques consists in free-interface normal modes, residual flexibility attachment modes, and rigid-body modes. Because the vibration behavior of unconstrained substructures is not under investigation, rigid-body modes are not included here. Therefore, the displacement vector can be expressed as

$$\boldsymbol{X}(t) = \boldsymbol{\Psi}\boldsymbol{F}_m(\boldsymbol{U}, \dot{\boldsymbol{U}}, t) + \boldsymbol{\Phi}\boldsymbol{q}(t) = \begin{bmatrix} \boldsymbol{\Psi} & \boldsymbol{\Phi} \end{bmatrix} \begin{Bmatrix} \boldsymbol{F}_m(\boldsymbol{U}, \dot{\boldsymbol{U}}, t) \\ \boldsymbol{q}(t) \end{Bmatrix} \tag{4}$$

where $\boldsymbol{\Psi}$ and $\boldsymbol{\Phi}$ are, respectively, $n \times n_{\mathrm{md}}$ matrix of the so-called residual flexibility attachment modes and $n \times n_{\mathrm{nm}}$ matrix of free-interface normal modes. The n_{md} and n_{nm} indicate the number of static modes corresponding to the number of master DOF and the number of normal modes kept in the projection basis, respectively. Vector $\boldsymbol{q}$ contains modal amplitudes.

Equation (4) is referred to as reduction equation in this paper because it represents the relation between physical DOF and generalized coordinates. Before moving to the next step, it is worth recalling the physical meaning of the set of modes in $\boldsymbol{\Phi}$ and $\boldsymbol{\Psi}$ for the reduction.

The free-interface modes $\boldsymbol{\Phi}$ retained in the projection basis are, in our case, a subset of mass-normalized modes of the substructure when linear DOF are kept free and contact pairs (nonlinear DOF) are not engaged (fully separate interfaces). The set of modes to be retained in the analysis is usually selected in a way that all the modes that might contribute to the dynamics of the system in the frequency range of interest are included in the model.

Attachment modes are the substructure static deformed shapes due to unit forces applied at master DOF and correspond to the columns of flexibility matrix $\boldsymbol{G}$ (i.e., the inverse of $\boldsymbol{K}$) related to master coordinates $\boldsymbol{G}^m$. The residual flexibility attachment modes $\boldsymbol{\Psi}$ (master coordinates-related columns of residual flexibility matrix) are obtained from the set of attachment mode matrix $\boldsymbol{G}^m$ by removing the contribution of the retained free-interface modes as

$$\boldsymbol{\Psi} = \boldsymbol{G}^m - \sum_{p=1}^{n_{\mathrm{nm}}} \frac{\boldsymbol{\phi}_p \boldsymbol{\phi}_{p,m}^T}{\omega_p^2} \tag{5}$$

where ω_p and $\boldsymbol{\phi}_{p,m}$ are the pth free-interface normal mode natural frequency and mode shape at master DOF. Considering residual flexibility attachment modes, the reduction basis provides two sets of spectrally orthogonal vectors $\boldsymbol{\Phi}$ and $\boldsymbol{\Psi}$, and therefore, as shown in [27], Eq. (4) can be directly used for forced response analysis, while this equation can be transformed to frequency domain using the MHB method because periodic displacements and forces are assumed, resulting in

$$\bar{\boldsymbol{X}}^{(h)} = \boldsymbol{\Psi}\bar{\boldsymbol{F}}_m^{(h)}(\bar{\boldsymbol{U}}) + \boldsymbol{\Phi}\bar{\boldsymbol{q}}^{(h)} = [\boldsymbol{\Psi} \quad \boldsymbol{\Phi}] \begin{Bmatrix} \bar{\boldsymbol{F}}_m^{(h)}(\bar{\boldsymbol{U}}) \\ \bar{\boldsymbol{q}}^{(h)} \end{Bmatrix} \tag{6}$$

The set of static and normal mode matrices can also be partitioned into two submatrices related to deflection at master and slave DOF:

$$\boldsymbol{\Phi} = \begin{bmatrix} \boldsymbol{\Phi}_m \\ \boldsymbol{\Phi}_s \end{bmatrix}, \qquad \boldsymbol{\Psi} = \begin{bmatrix} \boldsymbol{\Psi}_m \\ \boldsymbol{\Psi}_s \end{bmatrix} \tag{7}$$

allowing for efficient partitioning of the reduction equation, which will be exploited in the next sections.

In the following, the aforementioned reduction techniques are described, where Eqs. (1) and (4) are used to start the matrix projection and derivation of reduced equations.

1. *Rubin's Method*

Rubin's method [24] is used as a reference in this paper due to its high accuracy [29] when used to generate ROMs for the nonlinear forced response of structures with friction contacts, and due to its popularity, which makes it one of the CMS-based reduction methods available in all the commercial FE packages. According to Rubin's method, the governing equations of the system are projected on the subspace spanned by the columns of the reduction matrix defined in Eq. (4). As a result, the following reduced equations are obtained:

$$[-(h\omega)^2\boldsymbol{m} + ih\omega\boldsymbol{c} + \boldsymbol{k}]\bar{\boldsymbol{x}}^{(h)} = \bar{\boldsymbol{f}}^{(h)}, \quad h = 0, 1, \ldots, H \tag{8}$$

where the ROM matrices and vectors are defined as $\boldsymbol{m} = \boldsymbol{R}^T\boldsymbol{M}\boldsymbol{R}$, $\boldsymbol{c} = \boldsymbol{R}^T\boldsymbol{C}\boldsymbol{R}$, $\boldsymbol{k} = \boldsymbol{R}^T\boldsymbol{K}\boldsymbol{R}$, $\boldsymbol{x} = \boldsymbol{R}^T\boldsymbol{X}$, and $\boldsymbol{f} = \boldsymbol{R}^T\boldsymbol{F}$ with

$$\boldsymbol{R} = \begin{bmatrix} \boldsymbol{I} & \boldsymbol{0} \\ \boldsymbol{\Psi}_s\boldsymbol{\Psi}_m^{-1} & \boldsymbol{\Phi}_s - \boldsymbol{\Psi}_s\boldsymbol{\Psi}_m^{-1}\boldsymbol{\Phi}_m \end{bmatrix}$$

2. *Dual Formulation for Structures with Friction Contact*

A ROM suitable for nonlinear dynamic analysis of structures with contacts was presented recently in [27], where the idea of keeping interface forces in ROM is used. In this free-interface-based reduction technique, no reduced matrices are generated. To derive the reduced governing equations, the partition of Eq. (6) related to master DOF is extracted:

$$\bar{\boldsymbol{X}}_m^{(h)} = \boldsymbol{\Psi}_m\bar{\boldsymbol{F}}_m^{(h)}(\bar{\boldsymbol{U}}) + \boldsymbol{\Phi}_m\bar{\boldsymbol{q}}^{(h)} \tag{9}$$

The modal coordinates $\bar{\boldsymbol{q}}^{(h)}$ can be expressed as the following in frequency domain when a mass proportional damping $\boldsymbol{C} = \alpha\boldsymbol{M}$ is assumed:

$$\bar{\boldsymbol{q}}^{(h)} = \mathrm{diag}\left[\frac{1}{\omega_p^2 - \kappa^2}\right]\boldsymbol{\Phi}_m^T\bar{\boldsymbol{F}}_m^{(h)}(\bar{\boldsymbol{U}}), \quad h = 0,1,\ldots,H \tag{10}$$

The variable κ is defined as $\kappa^2 = (h\omega)^2 - i2\zeta_p\omega_p h\omega = (h\omega)^2 - i\alpha h\omega$, where ω_p and $\zeta_p = \alpha/(2\omega_p)$ are, respectively, the natural frequency and the damping ratio associated with the pth free-interface mode $\boldsymbol{\phi}_p$. Equation (10) is obtained by turning Eq. (2) into modal coordinates by writing the physical DOF as a linear combination of free-interface mode shapes $\boldsymbol{X} = \boldsymbol{\Phi}\boldsymbol{q}$ and by projecting the equations to the modal space premultiplying by $\boldsymbol{\Phi}^T$.

Finally, the response of the system is found by replacing $\bar{\boldsymbol{q}}^{(h)}$ in Eq. (10):

$$\bar{\boldsymbol{X}}_m^{(h)} = \boldsymbol{\Psi}_m\bar{\boldsymbol{F}}_m^{(h)}(\bar{\boldsymbol{U}}) + \boldsymbol{\Phi}_m\mathrm{diag}\left[\frac{1}{\omega_p^2 - \kappa^2}\right]\boldsymbol{\Phi}_m^T\bar{\boldsymbol{F}}_m^{(h)}(\bar{\boldsymbol{U}}), \quad h = 0, 1 \ldots, H \tag{11}$$

Because, similar to the DCB method that the forces for master DOF are kept as generalized coordinates and are not replaced by the displacements of master DOF, this formulation is referred to as Dual formulation. The two parts on the right side of this equation will be referred to as static and dynamic parts, respectively. It is notable that in the DCB method originally proposed for linear substructuring, compatibility constraints are explicitly expressed by an equality between corresponding DOF on the interfaces, while the resulting equations do not hold for substructures with friction interfaces because there is relative displacement between adjacent substructures. Therefore, in Dual formulation, on the contrary to the DCB method, the redundant constraint equations are not considered. Dual formulation is equal

to the one obtained by Petrov in [26] when the reference FRF matrix is calculated at zero frequency, although obtained via completely different approaches.

It is worth noting that the partition of residual flexibility attachment modes corresponding to master DOF $\boldsymbol{\Psi}_m$ can be obtained by importing master-related entries of free-interface normal modes and attachment modes from an FE software and computed as

$$\boldsymbol{\Psi}_m = \boldsymbol{G}_m^m - \boldsymbol{\Phi}_m \text{diag}\left[\frac{1}{\omega_p^2}\right]\boldsymbol{\Phi}_m^T \tag{12}$$

One drawback of the Dual formulation is neglecting the dynamic effects of residual flexibility attachment modes in the ROM, that is, the projection of mass and damping matrices on residual flexibility attachment modes is ignored. This stems from the projection of dynamic equation of motions [Eq. (1)] only on free-interface normal modes [Eq. (10)]. In other words, only stiffness matrix is projected on both sets of reduction basis that leads to nonconsistent projection. So, although the accuracy of this method is better than modal truncation method, as shown in [26], it is less accurate than other CMS reduction methods, and a larger ROM is usually required to predict the accurate response of the full structure [28].

3. UHR Method

The aim of this method is to take advantage of the positive features of all methods, including the small computational effort of Dual formulation as well as the accuracy of Rubin's ROM. Therefore, Galerkin projection of the dynamic equations of motion in frequency domain [Eq. (2)] is performed using reduction equation in frequency domain (Eq. (6) is replaced in Eq. (2), and then the resulting equations are premultiplied by $[\boldsymbol{\Psi}\ \boldsymbol{\Phi}]^T$.), which leads to

$$\begin{aligned}\boldsymbol{\Psi}^T\boldsymbol{D}^{(h)}\boldsymbol{\Psi}\bar{\boldsymbol{F}}_m^{(h)} &= \boldsymbol{\Psi}^T\bar{\boldsymbol{F}}^{(h)}\\ \boldsymbol{\Phi}^T\boldsymbol{D}^{(h)}\boldsymbol{\Phi}\bar{\boldsymbol{q}}^{(h)} &= \boldsymbol{\Phi}^T\bar{\boldsymbol{F}}^{(h)}\end{aligned} \tag{13}$$

where $\boldsymbol{D}^{(h)} = -(h\omega)^2\boldsymbol{M} + ih\omega\boldsymbol{C} + \boldsymbol{K}$ is the dynamic stiffness matrix of the full-order system corresponding to the hth harmonic. The orthogonal properties of normal modes and residual flexibility attachment modes result in the following equations by assuming a mass proportional damping $\boldsymbol{C} = \alpha\boldsymbol{M}$:

$$\begin{aligned}(-\kappa^2\boldsymbol{\Psi}^T\boldsymbol{M}\boldsymbol{\Psi} + \boldsymbol{\Psi}_m)\bar{\boldsymbol{F}}_m^{(h)} &= \boldsymbol{\Psi}^T\bar{\boldsymbol{F}}^{(h)}\\ \text{diag}[\omega_p^2 - \kappa^2]\bar{\boldsymbol{q}}^{(h)} &= \boldsymbol{\Phi}_m^T\bar{\boldsymbol{F}}_m^{(h)}\end{aligned} \tag{14}$$

In this step, the Fourier coefficients of forces at master DOF $\bar{\boldsymbol{F}}_m^{(h)}$ and modal coordinate $\bar{\boldsymbol{q}}^{(h)}$ can be computed using two sets of Eq. (13) as a function of projected dynamic stiffness matrix on reduction basis. To this end, the inverses of their coefficients on the left side of the two sets of equations are premultiplied in two sides of these equations, resulting in

$$\bar{\boldsymbol{F}}_m^{(h)} = (-\kappa^2\boldsymbol{\Psi}^T\boldsymbol{M}\boldsymbol{\Psi} + \boldsymbol{\Psi}_m)^{-1}\boldsymbol{\Psi}^T\bar{\boldsymbol{F}}^{(h)} \tag{15}$$

$$\bar{\boldsymbol{q}}^{(h)} = \text{diag}\left[\frac{1}{\omega_p^2 - \kappa^2}\right]\boldsymbol{\Phi}_m^T\bar{\boldsymbol{F}}_m^{(h)} \tag{16}$$

These two terms can be entered in Eq. (6) to obtain the final reduced governing equations. Thus, the displacement Fourier coefficients at master DOF are obtained as follows by considering that the entries of forces vector related to slave DOF are zero $\boldsymbol{F}_s = 0$:

$$\begin{aligned}\bar{\boldsymbol{X}}_m^{(h)} = {}& \boldsymbol{\Psi}_m(-\kappa^2\boldsymbol{\Psi}^T\boldsymbol{M}\boldsymbol{\Psi} + \boldsymbol{\Psi}_m)^{-1}\boldsymbol{\Psi}_m\boldsymbol{F}_m^{(h)}(\bar{\boldsymbol{U}})\\ &+ \boldsymbol{\Phi}_m\text{diag}\left[\frac{1}{\omega_p^2 - \kappa^2}\right]\boldsymbol{\Phi}_m^T\bar{\boldsymbol{F}}_m^{(h)}(\bar{\boldsymbol{U}})\end{aligned} \tag{17}$$

This formulation consists in two terms as Dual formulation [Eq. (11)], which are called again static and dynamic parts. The comparison of this upgraded formulation with the Dual formulation shows that the dynamic parts related to the projection of dynamic stiffness matrix on free-interface normal modes are identical. But, the static parts include two more terms, corresponding to the mass and damping matrix projection on static modes. As a consequence, the UHR is expected to perform better than the Dual formulation. The result of accuracy investigation is presented in Sec. III.A.1.

It is noteworthy that the dynamic effects of static modes are also included in the formulation obtained by Petrov in [26] when the reference FRF matrix is not calculated at zero frequency. The main difference of these two formulations is in the static part of UHR formulation, updated at each frequency, and the corresponding terms in Petrov formulation that are constant (calculated at a chosen frequency) over the frequency range. As a result, the Petrov formulation is exact at a given frequency and highly accurate in the frequency range close to that frequency.

Previous studies [28,31] have shown that Rubin's method performs better than other free-interface reduction techniques over a wide range of contact configurations, ranging from fully open to fully stuck contacts. The UHR formulation provides the same level of accuracy as Rubin's method by the consistent projection of equations of motion, while its off-line cost is smaller because of the decreased required computations. The result of accuracy investigation is presented in Secs. III.A.1 and III.B.

C. Nonlinear Forced Response Analysis

To find the nonlinear forced response of a structure with friction contact, the governing equations obtained by the MHB method and model order reduction techniques should be solved. These reduced equations in frequency domain are nonlinear because of the presence of nonlinear friction forces between the substructures. Therefore, an iterative solution method based either on the classic Newton–Raphson method [32] or on more advanced continuation algorithms is required.

Newton–Raphson method is used in this study, in which the Fourier coefficients of the displacements are the unknowns and are used to compute the Fourier coefficients of the contact forces at each iteration. Then, both sets of Fourier coefficients are introduced into the reduced set of nonlinear equations. This process is repeated until the equilibrium equations are satisfied and the residual r lies within a specified tolerance. The following relations are used for each reduction method to obtain the residual:

Dual: $\boldsymbol{r}^{(h)} = \bar{\boldsymbol{X}}_N^{(h)} - \boldsymbol{\Psi}_N\boldsymbol{F}_m^{(h)}(\bar{\boldsymbol{U}}) + \boldsymbol{\Phi}_N\text{diag}[\frac{1}{\omega_p^2-\kappa^2}]\boldsymbol{\Phi}_m^T\bar{\boldsymbol{F}}_m^{(h)}(\bar{\boldsymbol{U}})$

UHR: $\boldsymbol{r}^{(h)} = \bar{\boldsymbol{X}}_N^{(h)} - \boldsymbol{\Psi}_N(-\kappa^2\boldsymbol{\Psi}^T\boldsymbol{M}\boldsymbol{\Psi} + \boldsymbol{\Psi}_m)^{-1}\boldsymbol{\Psi}_m\boldsymbol{F}_m^{(h)}(\bar{\boldsymbol{U}}) + \boldsymbol{\Phi}_N\text{diag}[\frac{1}{\omega_p^2-\kappa^2}]\boldsymbol{\Phi}_m^T\bar{\boldsymbol{F}}_m^{(h)}(\bar{\boldsymbol{U}})$

Rubin's: $\boldsymbol{r}^{(h)} = \bar{\boldsymbol{x}}_N^{(h)} - (\boldsymbol{D}_{\text{NN}}^{(h)} - \boldsymbol{D}_{\text{NL}}^{(h)}\boldsymbol{D}_{\text{LL}}^{(h)-1}\boldsymbol{D}_{\text{ln}}^{(h)})^{-1}(\bar{\boldsymbol{f}}_N^{(h)} - \boldsymbol{D}_{\text{NL}}^{(h)}\boldsymbol{D}_{\text{LL}}^{(h)-1}\bar{\boldsymbol{f}}_L^{(h)})$ [27]

where $\boldsymbol{D}^{(h)} = -(h\omega)^2\boldsymbol{m} + ih\omega c + \boldsymbol{k}$.

The part of equations related to nonlinear DOF is solved in nonlinear solver, and then its response is used to find the displacements at linear DOF.

To compute the Fourier coefficients of contact forces from the Fourier coefficients of contact displacements, it is necessary to alternate from frequency to time and vice versa, via the AFT method proposed by Cameron and Griffin [30]. In detail, within the Newton–Raphson scheme, Fourier coefficients of displacements are used to compute periodic displacements in time domain by inverse discrete Fourier transform; then the periodic contact forces are computed by means of an appropriate contact model; and finally, the Fourier coefficients of the contact forces are computed by discrete Fourier transform (Fig. 1) and are injected in the nonlinear equations, casted in the frequency domain.

The core of the AFT method is a node-to-node contact model [33,34] to compute the contact forces (f_x, f_y, and f_z) at each contact node pair of the contact area for a given periodic relative displacement (u_x, u_y, and u_z). The contact models, available in the literature, rely on the use of either the penalty function method [35] or the Lagrange multipliers [36] in identifying the contact surface and imposing the kinematic contact constraints. These models assume that

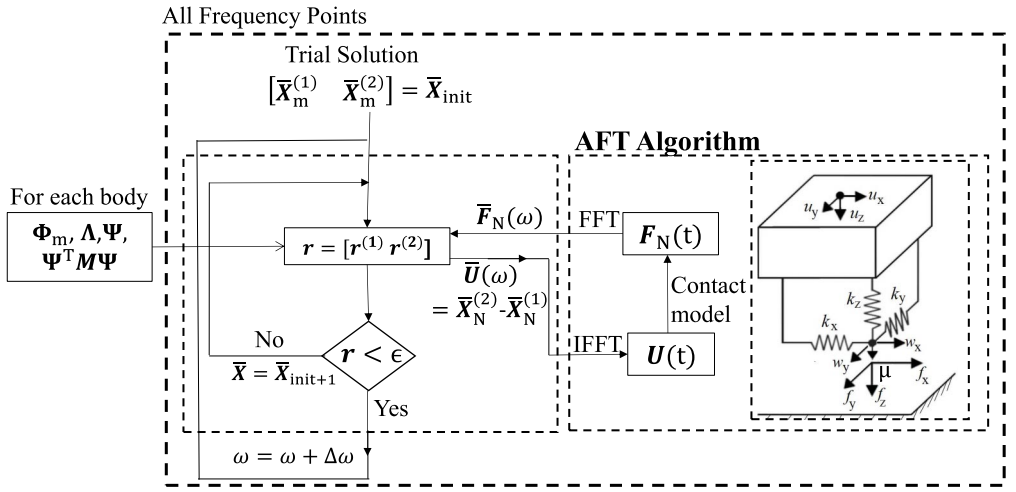

Fig. 1 Forced response analysis of two bodies with one contact surface, where 1 and 2 refer to body number.

1) Contact area mesh is small enough to have an adequate number of contact pairs that guarantee the accurate representation of dynamic behavior.

2) In the case of two bodies in contact, there are perfectly overlapped meshes on the contact surfaces so that node-to-node contact elements can be used.

A model based on penalty approach is used in this study, in which the contact interactions are split geometrically to normal and tangential directions where springs and Coulomb friction law are used to compute contact forces in alternate slip–stick–separation contact states.

A 3-D coupled contact model, addressed by Gu et al. [34] and Afzal et al. [37], is employed in this paper, which allows a coupled 2-D relative dimensional motion over the contact plane and a relative normal motion. Two tangential springs k_x and k_y and a normal spring k_z (Fig. 1) are defined to model the contact compliance. A friction coefficient μ is also assumed between the contact surfaces.

D. Computational Time

The computational time for forced response analysis of a reduced system can be divided into off-line time and online time.

Off-line time includes the time devoted to the generation of the ROM, and it is split into the time for 1) reduction basis computation and 2) reduced matrices generation (if needed). Reduction basis computation consists in four parts: 1) importation or construction of the full structural matrices, 2) solution of an eigenvalue problem to find the modal properties of full model, 3) a series of static analysis to find attachment modes, and 4) computation of residual flexibility attachment modes using Eq. (5).

The online time includes the solution time, including the iterative solution and the computation of harmonic components of friction forces through the AFT method. This cost is scaled by the number of nonlinear DOF (n_{nd}) [38]. The number of normal modes and the ability of the reduced model to reproduce the full system can also affect the online time. In detail, the online cost of the forced response analysis of a structure with distinct reduction methods, when the number of normal modes and nonlinear DOF are identical, is different, considering the ROM accuracy and the computation time of the residual in nonlinear solver for each reduction method.

For the dynamic analysis of industrial structures, a conventional FE analysis software is used as mesh generator. So, the modal properties ($\boldsymbol{\Phi}$, $\boldsymbol{\Lambda}$) and attachment modes ($\boldsymbol{G}^m$) of the substructures necessary in all the free-interface reduction methods analyzed in this paper can be computed in the FE software and exported for matrix manipulation and forced response analysis. The matrices of these FE models are very large, and exporting these models is time consuming.

In Fig. 2, a schematic of the three reduction processes is shown. The classical CMS methods, as Rubin's, require the full $\boldsymbol{M}$ and $\boldsymbol{K}$ matrices to be exported to compute the reduced matrices by projection, using the full vectors of attachment and normal modes. On the other side, the Dual formulation only requires master DOF entries of attachment and normal modes to define the balance equations of the ROM for nonlinear forced response. Finally, the UHR formulation lies in between the two aforementioned methods, because, although full $\boldsymbol{M}$ matrix and full attachment modes are needed, only master DOF entries of normal modes are necessary. As a result, the UHR formulation off-line cost is higher than the cost of Dual, but it is still smaller than Rubin's in both parts related to importing and computing the required elements. This formulation can be promising for the analysis of structure, in which the stiffness matrix is perturbed and the effects of perturbation are considered on the reduction basis used in the formulation. The computational efforts corresponding to the elements that are computed in the program are investigated for a case study, and the results are presented in Sec. III.A.2.

III. Application of the UHR Method

In Methodology (Sec. II), Rubin's, Dual, and UHR formulations for model order reduction of structures with friction contact are described. To assess the accuracy and the computational cost of the UHR formulation, it has been applied to two test cases, by using Dual and Rubin's formulations as references for efficiency and accuracy.

A simple two-rod model is first used to compare how the off-line costs of the three methods scale with respect to the size of the model and to the number of nonlinear DOF. In addition, a simplified shrouded bladed disk model (with cyclic symmetry boundary conditions) is employed to investigate the accuracy of the UHR formulation, proposed in this paper, and to compare it with the two reference methods.

When checking the performances of ROMs for nonlinear forced response analysis, the value of the contact stiffness plays an important

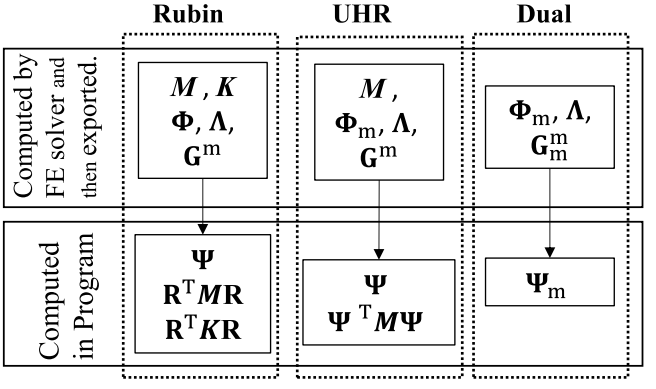

Fig. 2 Ingredients of the different reduction methods required for the generation of reduced nonlinear equations, which are imported to the program or computed in it.

role. On one side, too soft contacts do not allow to challenge free-interface reduction methods, as those described in this paper, because the mode shapes of structures with fully stuck contacts resemble those of the structures with open contacts. On the other hand, a too large value of contact stiffness affects the numerical convergence of the nonlinear solver. For the aforementioned reasons, in this paper, a tradeoff configuration was chosen: values of contact stiffness large enough to modify the mode shapes of the fully stuck system, without affecting the numerical convergence of the solution algorithm.

The performance of the ROMs is investigated in terms of resonance frequency and maximum vibration amplitude, using as a reference the full system response. In each analysis, a convergence analysis of the full system was performed to define the number of harmonics H. As an example, for the two-rod model (see Fig. 3) with $N_0/F = 20$ (stick-dominated regime), the convergence of the solution occurs when $H = 7$.

A. Two-Rod Model

The two-rod model (Fig. 4) corresponds to a structure with an inner contact. The structure is made of two rods, fixed at one end and in contact at the free end. Both rods use an isotropic linear elastic material model with properties given in Table 1.

Because the nodes in contact only experience tangential oscillation in axial direction, normal load (N_0) is constant, and consequently, the described 3-D coupled contact model is reduced to a 1-D contact model with constant normal load, as depicted in Fig. 4. So, a tangential contact stiffness $k = 2 \times 10^6$ N/m is used to model the local contact stiffness, and a coefficient of friction $\mu = 0.5$ is assumed.

As shown in Fig. 4, the first rod length is $2l$ and the second rod length is l with $l = 1$ m. The cross-sectional area of both rods is $A = 10$ mm^2. A periodic external force is also applied on midspan of the rod with length $2l$.

The forced response analysis of the two-rod model performed around the first resonance mode is shown in Fig. 5 for different N_0/F values, with the excitation $F = 100$ N and one contact element between the free ends of the rods.

Figure 5 shows the effects of contact condition on the forced response of structure with friction interfaces. This includes variations in resonance frequency and amplitude. With the highest value of N_0/F ratio, the system is in fully stuck condition, where bodies experience no slip and they behave linearly with an added stiffness between

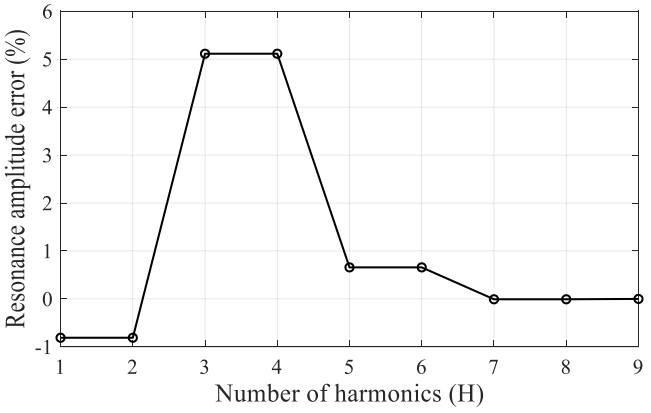

Fig. 3 Resonance amplitude error vs the number of harmonics (two-rod model; stick-dominated contact condition).

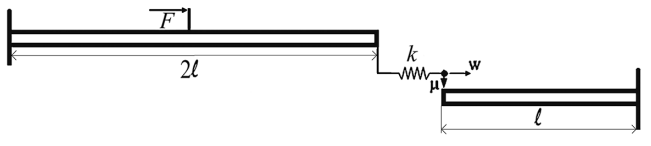

Fig. 4 Two-rod model test case with inner friction contact.

Table 1 Material properties of the rod model

Property	Value
Young's modulus E	70 GPa
Poisson's ratio ν	0.3
Density ρ	1000 kg/m^3
Mass proportional damping coefficient α	501/s

contact pairs. Decreasing the N_0/F ratio will change the contact state from full-stick condition toward stick-dominated regime, and then gross slip and eventually full separation. In stick-dominated regime, the contact node pair is mainly stuck during a period of vibration, but slip also occurs when friction force exceeds the limiting value. So, the resonance frequency is close to full-stick resonance frequency, but the peak amplitude is reduced due to energy dissipation during slip.

The studies about the accuracy and computational cost of the two-rod model are performed in stick-dominated regime contact condition. The reason is that this contact condition is usually considered as the design point of friction dampers because the response amplitude is lower than in the linear system and the resonance frequency has already stabilized. In addition, the nonlinear behavior of the structure in this condition seems as a severe case to capture for free-interface-based reduction methods that reduction basis includes the fully separate system modes [28,29].

This forced response analysis is performed with seven harmonics in Fourier series approximation of the periodic quantities. Higher harmonic components of friction forces can result in excitation of higher modes, and internal resonances can occur. Indeed, the energy transfer to higher modes (internal resonance) is the reason of multiple peaks that appeared in the forced response of the rod (Fig. 5). This can be well observed in this figure for $N_0/F = 1$ when the contact spends the largest amount of time in slip (slip-dominated regime) and nonlinearity is strong enough to generate large higher harmonic components of friction forces that can excite higher modes.

1. Accuracy

To assess the accuracy of the proposed reduction technique, the number of normal modes in the reduction basis is progressively increased. The convergence rate of the different ROMs is checked in the stick-dominated regime ($N_0/F = 20$) and shown in Fig. 6, in which the response curves are plotted, and in Fig. 7, in which the percentage errors of the ROM resonance frequency ($\varepsilon_f = 100\times |f_{\text{ROM}} - f_{\text{Full}}|/f_{\text{Full}}$) and amplitude ($\varepsilon_A = 100 \times |A_{\text{ROM}} - A_{\text{Full}}|/A_{\text{Full}}$) with respect to the full system response are plotted.

Figure 7 shows that the UHR and Rubin's formulations exhibit a more accurate prediction than Dual formulation, and a smaller reduced

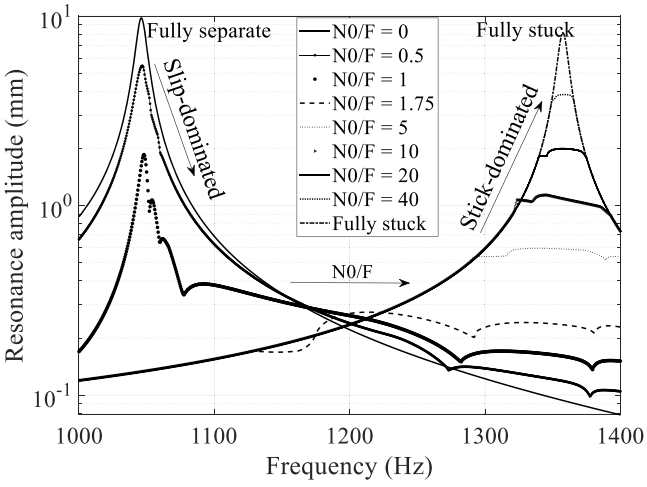

Fig. 5 Forced response of the rode with different values of static preload.

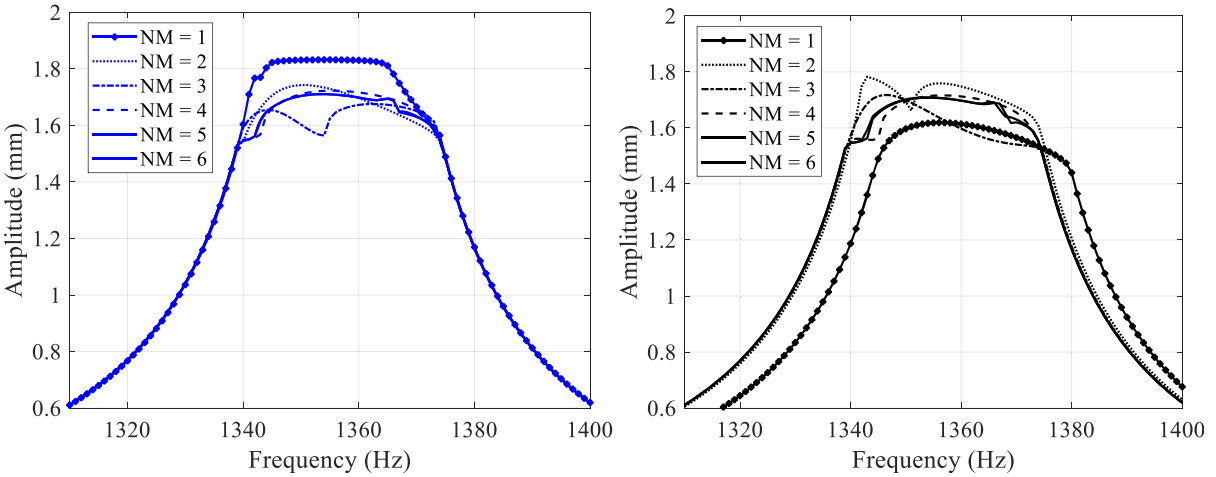

Fig. 6 Nonlinear response amplitude of the midlength DOF of rod 1: right, Dual; left, UHR and Rubin's.

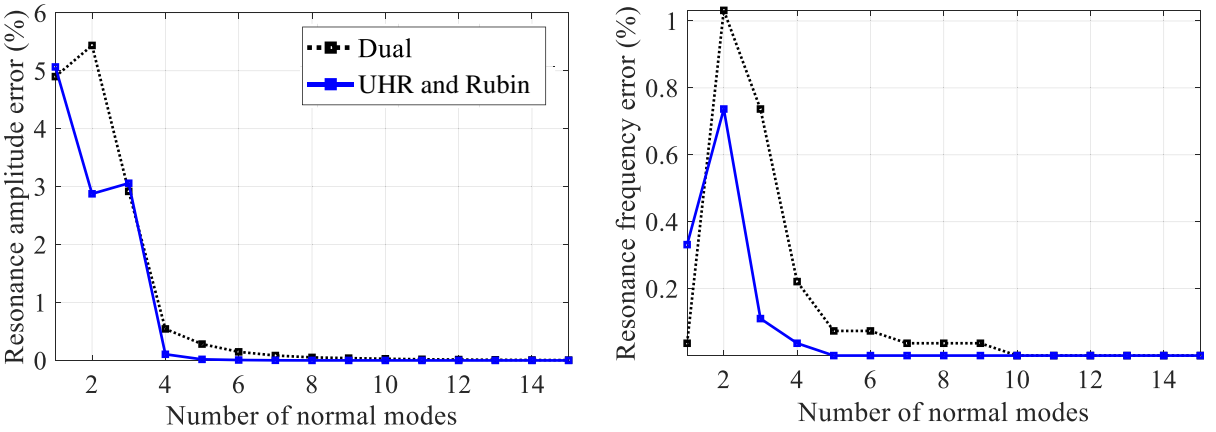

Fig. 7 Error of resonance frequency and amplitude obtained by ROMs with different numbers of normal modes.

model is required with these formulations. As explained in the Introduction, the reason of their better performance is the consistent projection, that is, all structural matrices are projected on the same basis; however, the projection of mass and damping matrices on the residual flexibility attachment modes is neglected in Dual formulation.

To better understand the free-interface normal mode effects on ROM convergence behavior in Fig. 7, the natural frequencies of the full-stick system (FS-f) are provided in Table 2 because the full-stuck system stiffness resembles the system stiffness in stick-dominated regime.

Table 2 shows that three mode natural frequencies are multiples of the first mode frequency that can be excited by internal resonance when the first mode is externally excited. However, the study of higher harmonic components of friction forces demonstrates that their even components are zero. Consequently, only the fifth mode can be internally excited.

Table 2 Resonance frequencies of two-rod model in fully stuck contact condition ($k = 2 \times 10^6$ N/m)

MN	FS-f, Hz	FS-f/1357.5
1	1,357.5	1.0
2	2,706.2	2.0
3	3,793.6	2.8
4	5,488.8	4.0
5	6,787.9	5.0
6	7,808.6	5.8
7	9,778.5	7.2
8	10,941.0	8.1

2. *Off-Line Cost*

The capability of the UHR formulation to accurately predict the forced response was shown in the previous section. To demonstrate the effectiveness of the UHR method, the computational effort is also evaluated by analyzing different FE models of the two-rod system, characterized by an increasing number of DOF. The evaluation is performed in terms of the off-line time. All FE models are reduced to ROMs with the same size. (The size of a reduced model is dependent on the number of normal modes and master DOF.)

As already mentioned in Sec. II.B, FE model generation as well as static and modal analyses necessary to obtain attachment and normal modes, needed in all the approaches analyzed in this paper, are computed in an FE commercial software in real applications. For these reasons, the computational cost related to those steps is not considered in the off-line cost comparison performed in this section. As a result, with reference to Fig. 2, the off-line costs only include time necessary to assemble the ROM vectors and matrices, which correspond to 1) Dual: $\boldsymbol{\Psi}_m$, 2) UHR: $\boldsymbol{\Psi}$ and $\boldsymbol{\Psi}^T\boldsymbol{M}\boldsymbol{\Psi}$, and 3) Rubin's: $\boldsymbol{\Psi}$, $\boldsymbol{R}^T\boldsymbol{M}\boldsymbol{R}$ and $\boldsymbol{R}^T\boldsymbol{K}\boldsymbol{R}$.

To assess the effect of the number of nonlinear DOF (n_{nd}) on off-line time, the analysis is performed first with one contact pair and increasing number of linear DOF, and then the number of nonlinear DOF is scaled proportionally with the number of linear DOF. The results are shown in Fig. 8, in which the time is normalized with respect to the off-line time of Rubin's method obtained by the largest model (total DOF = 35,000; $n_{\text{nd}} = 350$). In this figure, the off-line computing time of one rod vs the size of its FE model is depicted.

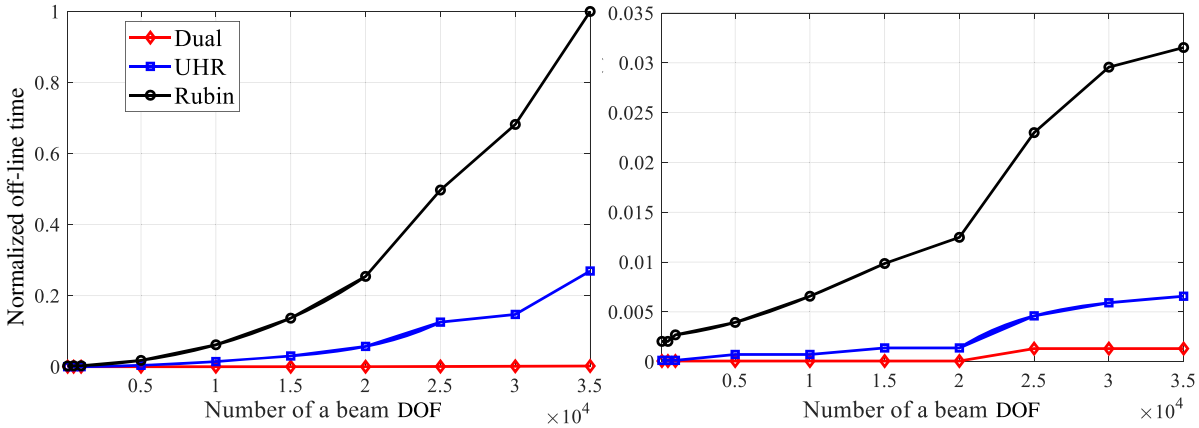

Fig. 8 ROM off-line computing time for models with different sizes when the number of nonlinear DOF is scaled (left) and constant (right).

It can be seen in Fig. 8 that the computational cost of Dual formulation is minimum. This time saving in addition to the low effort needed to only import master-DOF-related parts of static and dynamic modes is very important when the size of the FE model of the structure is considerably large and when the reduced model must be generated multiple times because of the variation of a structure parameter in design phase. This feature is significantly beneficial when the influence of the variation of this parameter can be directly applied to the $\boldsymbol{\Psi}_m$.

Figure 8 also illustrates the high dependency of the computational time of Rubin's method on the size of the model. The UHR off-line time is considerably smaller than Rubin's, although it is still higher than that of Dual. Regarding the UHR level of accuracy, this method can be particularly suitable in statistical analyses or optimization problems of high-fidelity FE models when more accuracy than Dual formulation is requested.

The significant effect of the n_{nd} can also be seen in Fig. 8 by comparing the left and right figures. The reason is that the n_{nd} in each model determines the number of attachment modes and the size of subsequent matrix multiplications.

The online cost associated to the frequency response analysis of the two-rod model is also shown in Table 3. This analysis is performed in stick-dominated contact condition described in Sec. III.A.1 ($N_0/F = 20$). Ten normal modes are kept in reduced model, while the analysis is once performed with one nonlinear DOF in a rod, and then with 10 nonlinear DOF to see the effects of n_{nd} on online time. The time shown in Table 3 is normalized with respect to the online time of the analysis with Rubin's reduced model and 10 nonlinear DOF.

Table 3 shows that the online time of the forced response analysis with Rubin's reduced model is higher than the time of analysis with UHR and Dual formulations when the size of the model is identical. This difference is related to the computational effort required to obtain the residual in nonlinear solver. The computation of the complement $(\boldsymbol{D}_{\text{NN}}^{(h)} - \boldsymbol{D}_{\text{NL}}^{(h)}\boldsymbol{D}_{\text{LL}}^{(h)-1}\boldsymbol{D}_{\text{ln}}^{(h)})^{-1}$ of the dynamics stiffness matrix either at each frequency (if the Newton–Raphson method is used) or at each iteration (if a continuation method is used) is very costly. The additional complement of the UHR formulation $\boldsymbol{\Psi}_N(-\kappa^2\boldsymbol{\Psi}^T\boldsymbol{M}\boldsymbol{\Psi} + \boldsymbol{\Psi}_m)^{-1}\boldsymbol{\Psi}_N$ compared to Dual formulation makes the cost of computing of UHR residual higher than that of Dual. But, the overall online time of UHR is a bit smaller than that of Dual in this study due to its higher accuracy and the consequent faster convergence of the nonlinear solver.

Table 3 Normalized online time of the frequency response analysis of the two-rod model in stick-dominated regime ($N_0/F = 20$)

	Reduction method		
n_{nd}	Dual	UHR	Rubin's
1	0.0328	0.0309	0.0328
10	0.7358	0.7311	1

B. Simplified Shrouded Blisk

An academic integrated turbine bladed disk (blisk) with friction contact between adjacent blade shrouds is considered as a second test case. This model, shown in Fig. 9, has 27 sectors with 17,268 DOF at each sector. Bladed disk material properties are Young's modulus $E = 200$ GPa, density $\rho = 7800$ kg/m^3, and Poisson's ratio of $\nu = 0.3$. Internal structural damping is introduced as mass proportional viscous damping, where $\alpha = 201/\text{s}$. The shroud contact nodes are in contact with adjacent blades; the nominal contact stiffness is $k = 5 \times 10^5$ N/m ($k_x = k_y = k_z = k$) and the friction coefficient is $\mu = 0.5$. The sectors are supposed to be identical, and therefore, cyclic symmetry boundary conditions are used.

With respect to the previous one, this test case represents a more realistic model with a more complicated dynamics. Each contact surface at the shroud comprises nine nonlinear contact nodes (54 nonlinear DOF). The forced response analysis is performed around the first resonance, corresponding to the first blade bending mode. The value of the N_0/F ratio is such that contact nodes are in microslip contact condition, the typical operating condition of shrouded bladed disk. Periodic external forces are modeled by a traveling-wave-type excitation with engine order 2.

In this analysis, the frequency responses are obtained for ROMs with different numbers of normal modes in reduction basis (Fig. 10). Five harmonics are retained in the Fourier expansion of periodic quantities.

The resonance amplitude and frequency are compared with the exact response, and the errors are depicted in Fig. 11.

Figure 11 shows that, in agreement with the rod model results, the UHR formulation provides much better performance. The Dual model needs more normal modes included in reduction basis to predict the response accurately due to ignorance of inertia and damping effects of residual flexibility attachment modes.

Table 4 provides more details about the convergence plots of Fig. 11. These resonance frequencies of the system show that the fourth mode can be excited by higher harmonic components of friction forces when the first mode is excited by external forces.

To better understand the nonlinear dynamics of this FE model and the convergence rate in Fig. 11, modal assurance criteria (MAC) plot of the first and fourth fully stuck modes with respect to the free-interface modes is shown in Fig. 12. This figure depicts that the first free-interface mode is very similar to the first full-stuck mode. Moreover, it is observed that the first four free-interface modes look similar to the fourth fully stuck modes, and the effect of these modes on the accuracy of the ROMs is clearly seen in Fig. 11. Because the first free-interface mode is similar to both the first and fourth fully stuck modes, UHR and Rubin's ROMs are able to give the exact value with only one mode in the reduced model.

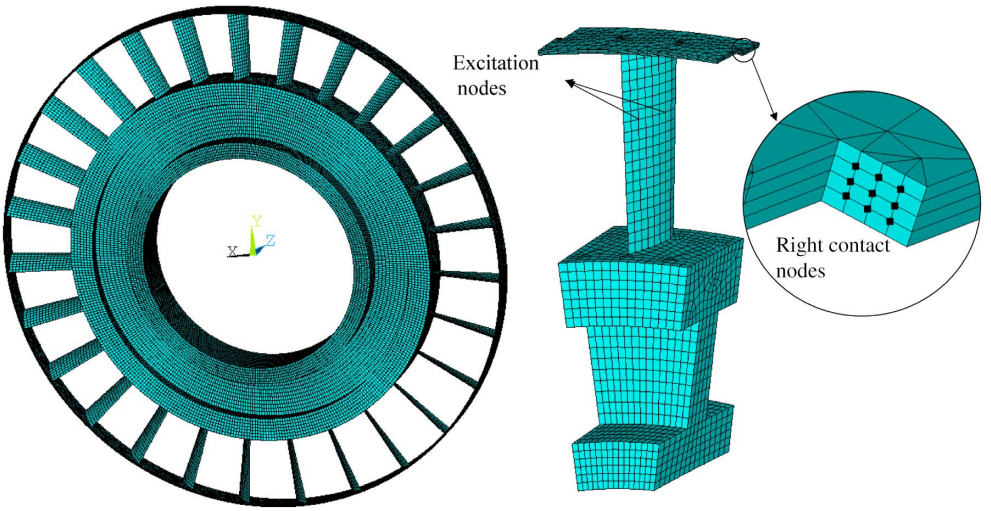

Fig. 9 FE model of the bladed disk and the single sector model.

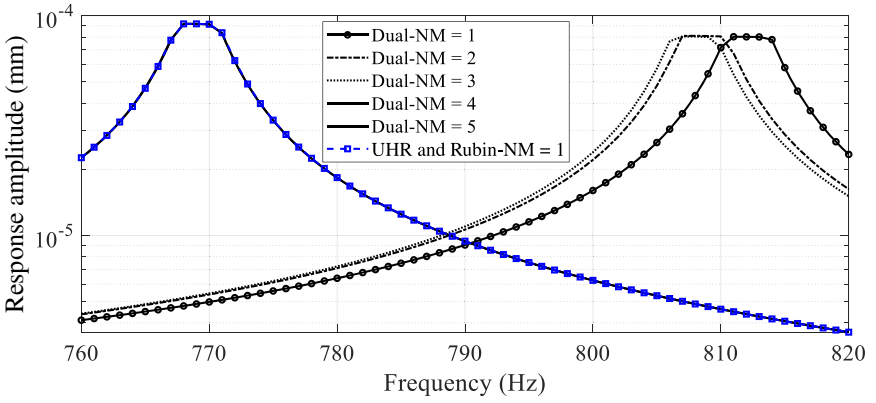

Fig. 10 Nonlinear response amplitude.

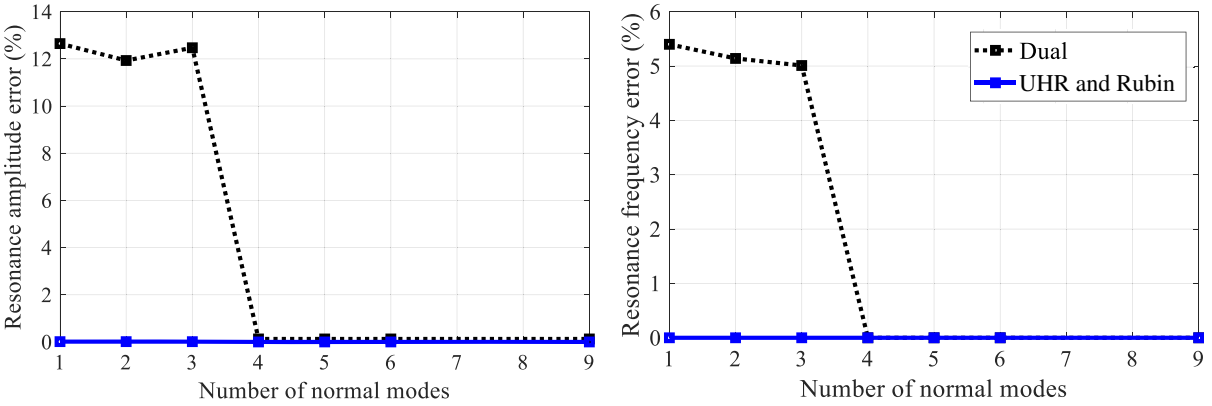

Fig. 11 Resonance frequency and amplitude error obtained by ROMs with different numbers of normal modes.

The computational cost of the analysis is also shown in Table 5. The off-line computing time is calculated, as stated in Sec. III.A.2. The online time refers to the forced response analysis of the reduced blisk model with 12 normal modes in microslip contact condition.

Both online and off-line times in Table 5 are normalized to the corresponding time obtained by Rubin's reduced model. This table demonstrates the effectiveness of the UHR formulation, because its computing time is considerably smaller than the time of Rubin's with the same level of accuracy as UHR.

IV. Conclusions

An upgraded reduced-order modeling technique for nonlinear forced response of a structure with friction contact is developed in this study. The method makes use of orthogonal properties of the residual flexibility attachment modes and of the free-interface modes. By the consistent projection of the structural matrices, the best accuracy is provided with low computational cost. The capabilities of this method in terms of accuracy and efficiency have been demonstrated on two test cases.

Table 4 Resonance frequencies of shrouded bladed disk model in fully stuck contact condition ($k = 5 \times 10^5$ N/m)

MN	FS-f, Hz	FS-f/769.1
1	769.1	1.0
2	1337.3	1.7
3	2966.8	3.9
4	3845.9	5.0
5	4864.1	6.3
6	6150.4	8.0
7	6235.5	8.1
8	7370.2	9.6

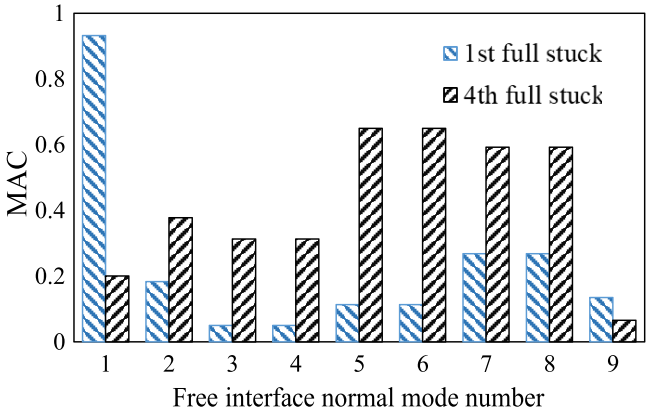

Fig. 12 Shrouded bladed disk MAC of the first and fourth fully stuck modes vs first nine free-interface modes.

Table 5 Computing cost of the nonlinear forced response analysis of the blisk model with different reduction methods

Reduction method	Dual	UHR	Rubin's
Normalized off-line time	0.004	0.25	1
Normalized online time	0.96	0.937	1

Because the derived model order reduction technique has small off-line computational cost and there is no need to full stiffness matrix, it is an interesting candidate for large industrial models, like mistuned bladed disk. This method can be especially beneficial for the statistical analysis of bladed disk with stiffness mistuning. The application of the proposed method for these cases can be further studied.

References

[1] Barrière, L., Marguet, S., Castanié, B., Cresta, P., and Passieux, J.-C., "An Adaptive Model Reduction Strategy for Post-Buckling Analysis of Stiffened Structures," *Thin-Walled Structures*, Vol. 73, Dec. 2013, pp. 81–93. https://doi.org/10.1016/j.tws.2013.07.009

[2] Yuan, J., El-Haddad, F., Salles, L., and Wong, C., "Numerical Assessment of Reduced Order Modeling Techniques for Dynamic Analysis of Jointed Structures with Contact Nonlinearities," *Journal of Engineering for Gas Turbines and Power*, Vol. 141, No. 3, 2019, Paper 031027. https://doi.org/10.1115/1.4041147

[3] Karim, Y., and Blanzé, C., "Vibration Reduction of a Structure by Design and Control of a Bolted Joint," *Computers & Structures*, Vol. 138, July 2014, pp. 73–85. https://doi.org/10.1016/j.compstruc.2014.02.009

[4] Zucca, S., Firrone, C. M., and Gola, M. M., "Numerical Assessment of Friction Damping at Turbine Blade Root Joints by Simultaneous Calculation of the Static and Dynamic Contact Loads," *Nonlinear Dynamics*, Vol. 67, No. 3, 2012, pp. 1943–1955. https://doi.org/10.1007/s11071-011-0119-y

[5] Corral, R., and Gallardo, J. M., "Nonlinear Dynamics of Bladed Disks with Multiple Unstable Modes," *AIAA Journal*, Vol. 52, No. 6, 2014, pp. 1124–1132. https://doi.org/10.2514/1.J051812

[6] Zucca, S., and Epureanu, B. I., "Reduced Order Models for Nonlinear Dynamic Analysis of Structures with Intermittent Contacts," *Journal of Vibration and Control*, Vol. 24, No. 12, 2018, pp. 2591–2604. https://doi.org/10.1177/1077546316689214

[7] Wang, X., O'Hara, P., Mignolet, M., and Hollkamp, J., "Reduced Order Modeling with Local Enrichment for the Nonlinear Geometric Response of a Cracked Panel," *AIAA Journal*, Vol. 57, No. 1, 2019, pp. 421–436. https://doi.org/10.2514/1.J057358

[8] Griffin, J., "Friction Damping of Resonant Stresses in Gas Turbine Engine Airfoils," *Journal of Engineering for Gas Turbines and Power*, Vol. 102, No. 2, 1980, pp. 329–333. https://doi.org/10.1115/1.3230256

[9] Gastaldi, C., and Berruti, T. M., "Competitive Time Marching Solution Methods for Systems with Friction-Induced Nonlinearities," *Applied Sciences*, Vol. 8, No. 2, 2018, p. 291. https://doi.org/10.3390/app8020291

[10] Cardona, A., Coune, T., Lerusse, A., and Geradin, M., "A Multiharmonic Method for Non-Linear Vibration Analysis," *International Journal for Numerical Methods in Engineering*, Vol. 37, No. 9, 1994, pp. 1593–1608. https://doi.org/10.1002/nme.1620370911

[11] Sanliturk, K., and Ewins, D., "Modelling Two-Dimensional Friction Contact and Its Application Using Harmonic Balance Method," *Journal of Sound and Vibration*, Vol. 193, No. 2, 1996, pp. 511–523. https://doi.org/10.1006/jsvi.1996.0299

[12] Siewert, C., Panning, L., Wallaschek, J., and Richter, C., "Multiharmonic Forced Response Analysis of a Turbine Blading Coupled by Nonlinear Contact Forces," *Journal of Engineering for Gas Turbines and Power*, Vol. 132, No. 8, 2010, Paper 082501. https://doi.org/10.1115/1.4000266

[13] Mitra, M., Zucca, S., and Epureanu, B. I., "Adaptive Microslip Projection for Reduction of Frictional and Contact Nonlinearities in Shrouded Blisks," *Journal of Computational and Nonlinear Dynamics*, Vol. 11, No. 4, 2016, Paper 041016. https://doi.org/10.1115/1.4033003

[14] Craig, R., and Bampton, M., "Coupling of Substructures for Dynamic Analyses," *AIAA Journal*, Vol. 6, No. 7, 1968, pp. 1313–1319. https://doi.org/10.2514/3.4741

[15] Hanle, U., Dinkler, D., and Kroplin, B., "Interaction of Local and Global Nonlinearities of Elastic Rotating Structures," *AIAA Journal*, Vol. 33, No. 5, 1995, pp. 933–937. https://doi.org/10.2514/3.12659

[16] Charleux, D., Gibert, C., Thouverez, F., and Dupeux, J., "Numerical and Experimental Study of Friction Damping Blade Attachments of Rotating Bladed Disks," *International Journal of Rotating Machinery*, Vol. 2006, July 2006, Paper 071302. https://doi.org/10.1155/IJRM/2006/71302

[17] Petrov, E., and Ewins, D., "Effects of Damping and Varying Contact Area at Blade-Disk Joints in Forced Response Analysis of Bladed Disk Assemblies," *Journal of Turbomachinery*, Vol. 128, No. 2, 2006, pp. 403–410. https://doi.org/10.1115/1.2181998

[18] Géradin, M., and Rixen, D. J., "A 'Nodeless' Dual Superelement Formulation for Structural and Multibody Dynamics Application to Reduction of Contact Problems," *International Journal for Numerical Methods in Engineering*, Vol. 106, No. 10, 2016, pp. 773–798. https://doi.org/10.1002/nme.5136

[19] Pichler, F., Witteveen, W., and Fischer, P., "Reduced-Order Modeling of Preloaded Bolted Structures in Multibody Systems by the Use of Trial Vector Derivatives," *Journal of Computational and Nonlinear Dynamics*, Vol. 12, No. 5, 2017, Paper 051032. https://doi.org/10.1115/1.4036989

[20] Witteveen, W., and Irschik, H., "Efficient Mode Based Computational Approach for Jointed Structures: Joint Interface Modes," *AIAA Journal*, Vol. 47, No. 1, 2009, pp. 252–263. https://doi.org/10.2514/1.38436

[21] Yuan, J., Salles, L., El Haddad, F., and Wong, C., "An Adaptive Component Mode Synthesis Method for Dynamic Analysis of Jointed Structure with Contact Friction Interfaces," *Computers & Structures*, Vol. 229, March 2020, Paper 106177. https://doi.org/10.1016/j.compstruc.2019.106177

[22] MacNeal, R. H., "A Hybrid Method of Component Mode Synthesis," *Computers & Structures*, Vol. 1, No. 4, 1971, pp. 581–601. https://doi.org/10.1016/0045-7949(71)90031-9

[23] Martinez, D., Carne, T., Gregory, D., and Miller, A., "Combined Experimental/Analytical Modeling Using Component Mode Synthesis," *25th Structures, Structural Dynamics and Materials Conference*, AIAA Paper 1984-0941, May 1984. https://doi.org/10.2514/6.1984-941

[24] Rubin, S., "Improved Component-Mode Representation for Structural Dynamic Analysis," *AIAA Journal*, Vol. 13, No. 8, 1975, pp. 995–1006. https://doi.org/10.2514/3.60497

[25] Rixen, D. J., "A Dual Craig–Bampton Method for Dynamic Substructuring," *Journal of Computational and Applied Mathematics*, Vol. 168, Nos. 1–2, 2004, pp. 383–391. https://doi.org/10.1016/j.cam.2003.12.014

[26] Petrov, E., "A High-Accuracy Model Reduction for Analysis of Nonlinear Vibrations in Structures with Contact Interfaces," *Journal of Engineering for Gas Turbines and Power*, Vol. 133, No. 10, 2011, Paper 102503. https://doi.org/10.1115/1.4002810

[27] Zucca, S., "On the Dual Craig–Bampton Method for the Forced Response of Structures with Contact Interfaces," *Nonlinear Dynamics*, Vol. 87, No. 4, 2017, pp. 2445–2455. https://doi.org/10.1007/s11071-016-3202-6

[28] Mashayekhi, F., Zucca, S., and Nobari, A. S., "A Comparison of Two Reduction Techniques for Forced Response of Shrouded Blades with Contact Interfaces," *Dynamics of Coupled Structures*, Vol. 4, Springer, Cham, 2018, pp. 79–88. https://doi.org/10.1007/978-3-319-74654-8_7

[29] Mashayekhi, F., Zucca, S., and Nobari, A. S., "Evaluation of Free Interface-Based Reduction Techniques for Nonlinear Forced Response Analysis of Shrouded Blades," *Proceedings of the Institution of Mechanical Engineers, Part C: Journal of Mechanical Engineering Science*, Vol. 233, Nos. 23–24, 2019, pp. 7459–7475. https://doi.org/10.1016/j.tws.2013.07.009

[30] Cameron, T., and Griffin, J., "An Alternating Frequency/Time Domain Method for Calculating the Steady-State Response of Nonlinear Dynamic Systems," *Journal of Applied Mechanics*, Vol. 56, No. 1, 1989, pp. 149–154. https://doi.org/10.1115/1.3176036

[31] Gruber, F. M., and Rixen, D. J., "Evaluation of Substructure Reduction Techniques with Fixed and Free Interfaces," *Strojniški vestnik–Journal of Mechanical Engineering*, Vol. 62, No. 7, 2016, pp. 452–462. https://doi.org/10.5545/sv-jme.2016.3735

[32] Kelley, C. T., *Solving Nonlinear Equations with Newton's Method*, Vol. 1, Soc. for Industrial and Applied Mathematics, Philadelphia, 2003, pp. 1–25. https://doi.org/10.1137/1.9780898718898

[33] Yang, B., and Menq, C., "Characterization of 3D Contact Kinematics and Prediction of Resonant Response of Structures Having 3D Frictional Constraint," *Journal of Sound and Vibration*, Vol. 217, No. 5, 1998, pp. 909–925. https://doi.org/10.1006/jsvi.1998.1802

[34] Gu, W., Xu, Z., and Liu, Y., "A Method to Predict the Non-Linear Vibratory Response of Bladed Disc System with Shrouded Dampers," *Proceedings of the Institution of Mechanical Engineers, Part C: Journal of Mechanical Engineering Science*, Vol. 226, No. 6, 2012, pp. 1620–1632. https://doi.org/10.1177/0954406211424671

[35] Kikuchi, N., and Oden, J. T., *Contact Problems in Elasticity: A Study of Variational Inequalities and Finite Element Methods*, Vol. 8, Soc. for Industrial and Applied Mathematics, Philadelphia, 1988, pp. 49–54. https://doi.org/10.1137/1.9781611970845

[36] Radi, B., Baba, O., and Gelin, J.-C., "Treatment of the Frictional Contact via a Lagrangian Formulation," *Mathematical and Computer Modelling*, Vol. 28, Nos. 4–8, 1998, pp. 407–412. https://doi.org/10.1016/S0895-7177(98)00130-7

[37] Afzal, M., Arteaga, I. L., and Kari, L., "An Analytical Calculation of the Jacobian Matrix for 3D Friction Contact Model Applied to Turbine Blade Shroud Contact," *Computers & Structures*, Vol. 177, Dec. 2016, pp. 204–217. https://doi.org/10.1016/j.compstruc.2016.08.014

[38] Poudou, O., and Pierre, C., "Hybrid Frequency-Time Domain Methods for the Analysis of Complex Structural Systems with Dry Friction Damping," *44th AIAA/ASME/ASCE/AHS/ASC Structures, Structural Dynamics, and Materials Conference*, AIAA Paper 2003-1411, April 2003. https://doi.org/10.2514/6.2003-1411

R. K. Kapania
Associate Editor